Article ID: 1003-6326(2004)04-0675-06

Novel algorithm for determining optimal blankholder forces in deep drawing of aluminum alloy sheet①

SUN Cheng-zhi(孙成智), CHEN Guan-long(陈关龙), LIN Zhong-qin(林忠钦), ZHAO Yi-xi(赵亦希)
(School of Mechanical Engineering, Shanghai Jiaotong University, Shanghai 200030, China)

Abstract: Wrinkling and fracture are main defects in sheet metal forming of aluminum alloy sheet, which can be reduced or even eliminated by manipulating a suitable blank-holder forces (BHF). But, it is difficult to attain the optimum BHF during sheet metal forming. A new optimization algorithm integrating the finite element method (FEM) and adaptive response surface method is presented to determinate the optimal BHFs in deep drawing of aluminum rectangular box. To assure convergence, the trust region modes management strategies are used to adjust the move limit of design spaces. Finally, the optimum results of rectangular box deep drawing are given. Verification experiments are performed to verify the optimal result.

Key words: aluminum alloy sheets; blank-holder force; optimization; sheet metal forming

CLC number: TG 386 **Document code:** A

1 INTRODUCTION

The need to improve fuel economy and reduce emissions is an opportunity to expand the automotive applications of aluminum. But, aluminum sheet has poorer formability than steel sheet from both the wrinkling and tearing point of view. Much investigation shows that the formability of aluminum alloy can be improved by controlling process parameters[1, 2]. Among various process control methods, manipulation of the restraining force in the sheet during stamping has been proved to be the most effective method to increase formability of the sheet metal. But, the determination of BHFs is still very difficult, because sheet metal forming involves complex deformation[3-6]. With the advances of Computer-Aided Design and Engineering (CAD/CAE) techniques, computation-intensive numerical simulations are often used to more accurately study the deformation behavior from many aspects and to guide design improvements. However, the high computational cost associated with these analyses and simulations prohibits them from being used as performance measurement tools in the optimization of a design. The design optimization process normally requires a large number of numerical iterations, and each with one or more analysis calls before the optimal solution is identified. Therefore, the use of approximation models to replace the expensive computer analysis is an acturial approach to avoid the computation barrier to the application of modern CAD/CAE tools in design optimization[6-9]. A number of approximation methods have been introduced in the past. Among them the Response Surface Method (RSM) has attracted a growing interest in recent years[10]. The RSM is one of the designs of experiments (DOE) methods used to approximate an unknown function for which only a few values are computed. When experiments are expensive, the number of experiments required for the optimization must be minimized to reduce the total cost of the optimization. But, one-time RSM uses a first or second order regression model to approximate a complex design function that is often in a higher order form, leading to significant modeling errors over the design space[11].

A new method presented in this paper was introduced to determine the optimum BHFs during deep drawing process, and the method integrates the finite element method with Adaptive Response Surface Methodology (ARSM) based trust region modes management strategies. The optimum process parameters are determined to satisfy the given objective function for the desired strain state in the Forming Limit Diagram (FLD). The validity of the present algorithm is demonstrated with the determination procedure of the optimum BHF in rectangular box deep drawing.

2 DESIGN OF OPTIMIZATION PROCESS

2.1 Objective function

We define an objective function based on the Forming Limit Diagram (FLD), because it is consid-

① **Foundation item:** Project (50225520) supported by the National Natural Science Foundation of China for Distinguished Young Scholars

Received date: 2003-10-15; **Accepted date:** 2004-02-04

Correspondence: SUN Cheng-zhi, PhD; Tel: +86-21-62932125; E-mail: sun_chengzhi@163.com

ered as a good indicator for the fracture and wrinkling criteria. In order to evaluate the formability, we first define the Forming Limit Curve by an explicit function based on the least squares polynomial approximation. The function takes the form as follows:

$$\varepsilon_1=\varphi(\varepsilon_2)=\begin{cases}A_0+A_1\varepsilon_2+A_2\varepsilon_2^2, & \varepsilon_2\leqslant 0\\ A_3+A_4\varepsilon_2+A_5\varepsilon_2^2, & \varepsilon_2>0\end{cases}\tag{1}$$

where $A_1, \cdots, A_5$ are the coefficients.

Based on this function, a so called "secure FLC" function is defined as follows:

$$\Psi(\varepsilon_2)=\varphi(\varepsilon_2)-\Delta\tag{2}$$

where Δ is a "safety margin" from the FLC, a constant quantity chosen by the user, commonly 10%.

We define $\varepsilon_1=\Phi(\varepsilon_2)$ as wrinkling limit curve (the pure shear strain state $\rho=-1$).

Our objective function is thus expressed in terms of the distances from $\psi(\varepsilon_1, \varepsilon_2)$ but only for the elements where the major strain is greater than $\psi(\varepsilon_1, \varepsilon_2)$ and the distances from $\Phi(\varepsilon_1, \varepsilon_2)$ but only for the elements where the major strain is lower than $\Phi(\varepsilon_1, \varepsilon_2)$, see Fig. 1. Therefore the global objective function can be given by

$$f(\varepsilon_1, \varepsilon_2)=\alpha\sum(j_w^i)^2+\sum(j_F^i)^2\tag{3}$$

$$j_w^i=|\Phi(\varepsilon_2^e)-\varepsilon_1^e|, \quad \varepsilon_1^e\leqslant\Phi(\varepsilon_2^e)$$

$$j_F^i=|\varepsilon_1^e-\Psi(\varepsilon_2^e)|, \quad \varepsilon_1^e>\Psi(\varepsilon_2^e)$$

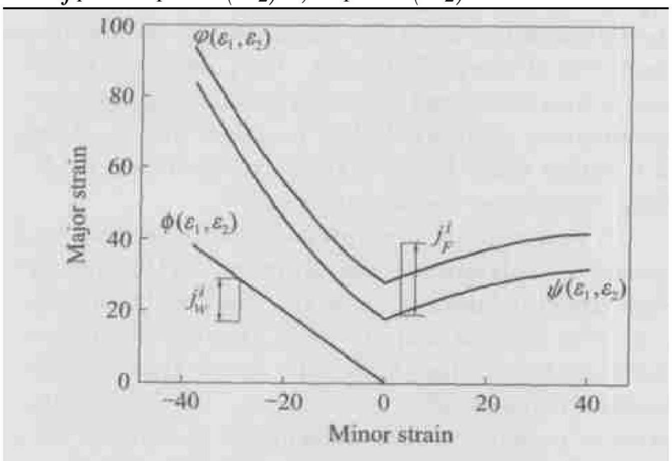

Fig. 1 Definition of objective function

The factor of α ($\alpha=0.1$) is determined by test runs to balance the contributions of two parts in the objective function. It should be pointed out that the formulation of the objective function is problem dependent and test runs are needed to verify the behavior of the objective function and the effectiveness of available optimization algorithms. During sheet metal forming, the smaller the objection function $f(\varepsilon_1, \varepsilon_2)$, the better the formability.

2.2 Design variables

For the rectangular box deep drawing, the blank-holder forces in different regions on the flange are selected as design variables. In order to obtain different BHFs in each region, a special blankholder is designed as shown in Fig. 2. Considering the symmetry, only BHF1 − BHF6 are selected as design variables.

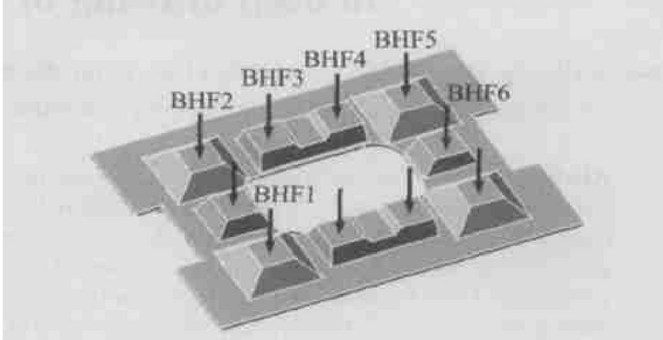

Fig. 2 Elastic blankholder

3 OPTIMIZATION PROCEDURE

3.1 Selection of design of experiment

Latin Hypercube Design (LHD) was introduced in present investigation. Because the LHD comes from a controlled random sampling method, inherited design is still random even in a reduced design space. The nature of the randomness is still maintained, which ensures the obtained response surface approximates the actual function equally across the design space. As a result, the total number of designs can be greatly reduced[12]. Mathematically, suppose that $(F_1, \cdots, F_d)$ are the distribution functions of the independent input variable $(x_1, \cdots, x_d)$ and x_{ij} is the ith value of the jth variable x_j for $i=1, \cdots, n$, $j=1, \cdots, d$. Define $\boldsymbol{p}=(p_{ij})$ to be an $n\times d$ matrix, where each column of $\boldsymbol{p}$ is an independent random permutation of $(1, \cdots, n)$. Moreover, let r_{ij} be $n\times d$ values of uniform [0, 1] random variables independent of $\boldsymbol{p}$. Then the design sites x_{ij} of a Latin hypercube sample are defined by

$$x_{ij}=F^{-1}\left|\frac{1}{n}(p_{ij}-r_{ij})\right|\tag{4}$$

where F^{-1} represents the inverse of the target cumulative distribution function, $p_{i1}, \cdots, p_{id}$ determine in which 'cell' x_{ij} is located, and $r_{i1}, \cdots, r_{id}$ determine where the 'cell' x_{ij} is located. In this work, all the distribution functions, F, are assumed to be uniform. There is still much freedom in assigning levels to dimensions and therefore numerous feasible LHDs exist. In order to capture the nature of actual system response, the sampling points should be distributed in whole design spaces (filling spaces). As a measure for the space-filling of a simulation scheme, we take the minimal distance between its two design points. The larger this minimal distance is, the better the simulation scheme is. Simulated Annealing (SA) algorithm is used to get the optimum design points which keep space filling design.

3.2 Approximation models

Two main alternatives have been investigated in approximate physical systems. The first approach has been the use of a simplified representation of the complicated physical system to obtain less costly simulations. The other for system approximation which has grown in interest in recent years, is response surface approximation methodology based on polynomial and interpolation models[13]. Polynomial RSA employs the statistical techniques of regression analysis and analysis of variance (ANOVA) to determine the approximate function. Consider a function $f(x)$ of n_eth design variables, for which its value is known

n_e at design sites. A quadratic model, $f(x)$, of the function $f(x)$ at the pth design site is given by

$$f^{(p)} = \beta_0 + \sum_{i=1}^{n_e} \beta_i x_i^{(p)} + \sum_{i=1}^{n_e}\sum_{j=1}^{n_e} \beta_{ij} x_i^{(p)} x_j^{(p)}$$

where $p = 1, \cdots, n_e$, $x_i^{(p)}$ and $x_j^{(p)}$ are the design variables at the pth site; β_0, β_i, and β_{ij} are the unknown polynomial coefficients which can be obtained from a least-squares method. Suppose $f^{(p)}$ is the pth observation.

3.3 Trust region modes management strategies

Trust region methods were originally introduced to apply to modern nonlinear unconstrained optimization algorithms to assure a robust global behavior. Robust global behavior infers the mathematical assurance that the optimization algorithm will converge to an initial iteration[14, 15]. In trust region methods, a

second-order approximation, $f(x)$, of the objective $f(x)$, is successively minimized with the trust region regulating the length of the steps in each iteration. On the other hand, the length of the steps or size of the trust region is controlled based on how well the quadratic model predicts the decrease in $f(x)$. A reliability index, $\rho_{(s)}$, which monitors how well the current approximation represents the actual design space is defined as

$$\rho_{(s)} = \frac{f(x^s) - f(x^{s+1})}{f(x^s) - f(x^{s+1})} \tag{6}$$

This is simply the ratio of the actual change in the function to the change predicted by the approximation.

After each optimization iteration, the trust region radius is updated according to the following principles:

1) $\rho_k \leqslant 0$

The surrogates are inaccurate. Reject the kth optimum x_*^k and let $x_c^{k+1} = x_c^k$, shrink the trust region by a factor of 0.25 to improve surrogate function accuracy.

2) $0 < \rho_k \leqslant 0.25$

The surrogates are marginally accurate. Let $x_c^{k+1} = x_*^k$, but shrink the trust region size by a factor 0.5 for the $(k+1)$th iteration.

3) $0.25 < \rho_k \leqslant 0.75$

The surrogates are moderately accurate. Let $x_c^{k+1} = x_*^k$ and maintain the current trust region size.

4) $\rho_k \geqslant 0.75$ and $\| x_*^{k+1} - x_c^k \| \leqslant \Delta^k$

The surrogates are accurate and x_*^k lies inside the trust region bounds. Let $x_c^{k+1} = x_*^k$ and maintain the current trust region size.

5) $\rho_k \geqslant 0.75$ and $\| x_*^{k+1} = x_c^k \| = \Delta^k$

The surrogates are accurate and x_*^k lies on the trust region bounds. Let $x_c^{k+1} = x_*^k$ and increase the trust region size by a factor of 2.

3.4 Termination criterion

During the simulation-based optimization, the search process terminates when the difference between the upper bound and the low bound for all variables or the relative variation of objective function becomes negligible. The termination criterion can be written as follows:

$$| x_L^i - x_U^i | \leqslant \varepsilon \quad (k = 1, \cdots, n) \tag{7}$$

where ε is specified by the designer.

The flow chart of adaptive response surface methodology optimization process is shown in Fig. 3.

4 NUMERICAL RESULTS

The optimization method is applied to the optimum BHF (around the flange) in rectangular box deep drawing for improving the formability. The geometry of the tools is presented in Fig. 4. Material properties of Al5052H32 are shown as follows: initial blank 400 mm × 300 mm, elastic modulus $E = 71.5$ GPa, initial thickness $h_0 = 1.6$ mm, anisotropic coefficient $r = 0.86$, friction coefficient $\mu = 0.12$, and a stress—strain curve is shown in Fig. 5.

Due to the symmetry of the problem, only half of the box is meshed with 1 268 nodes and 1 263 elements (Fig. 6). The optimization procedure exposed in pervious sections is applied to determine the optimal BHF minimizing the objective function. The number of iterations required to arrive at the final optimized design is 98. Table 1 lists the initial and optimum BHF, Fig. 7 shows the variation of the objective function, Fig. 8 and Fig. 9 illustrate the improvement in formability resulted from the optimization.

Table 1 Optimum results of rectangular box deep drawing

Parameters	BHF1/kN	BHF2/kN	BHF3/kN	BHF4/kN	BHF5/kN	BHF6/kN
Initial BHFs	2.0	2.0	2.0	2.0	2.0	2.0
Initial trust region radius	2.0	2.0	2.0	2.0	2.0	2.0
Optimum BHFs	1.4	1.1	1.6	2.5	1.5	1.6

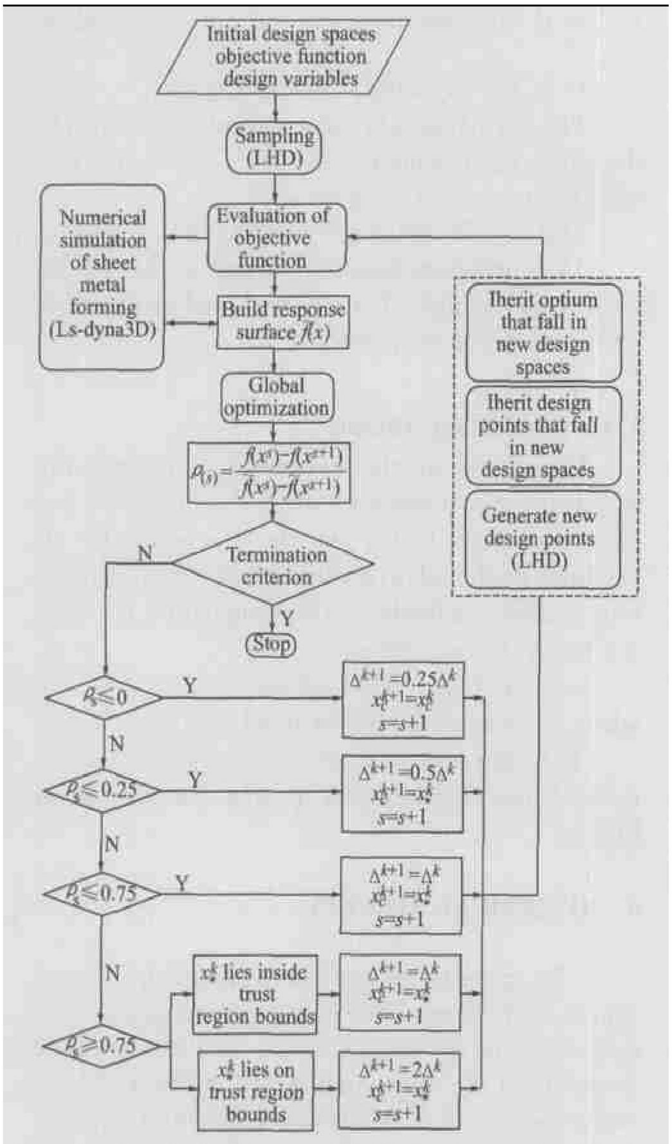

Fig. 3 Adaptive response surface methodology optimization process

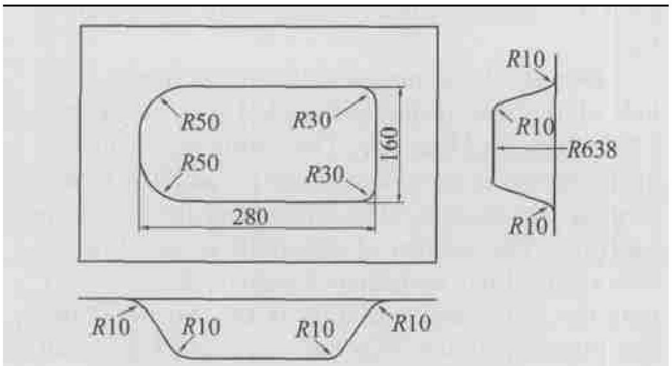

Fig. 4 Dimensions of rectangle

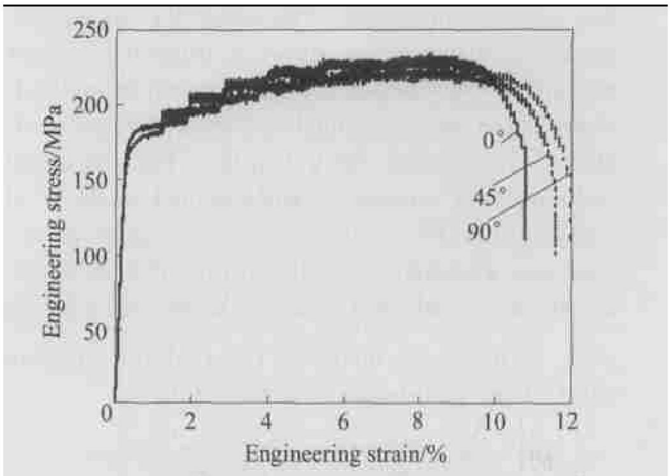

Fig. 5 Stress-strain curves of Al5052H32

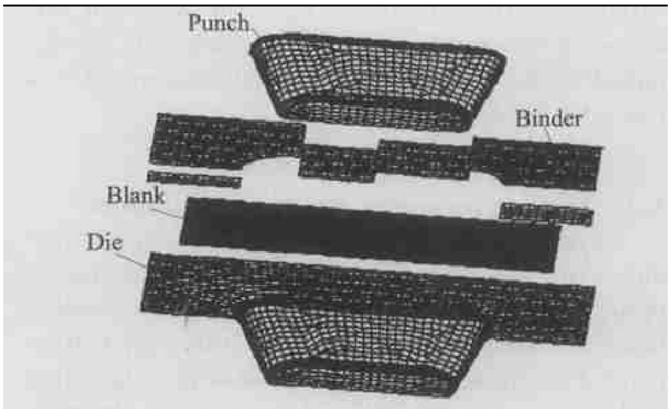

Fig. 6 Mesh of FEM

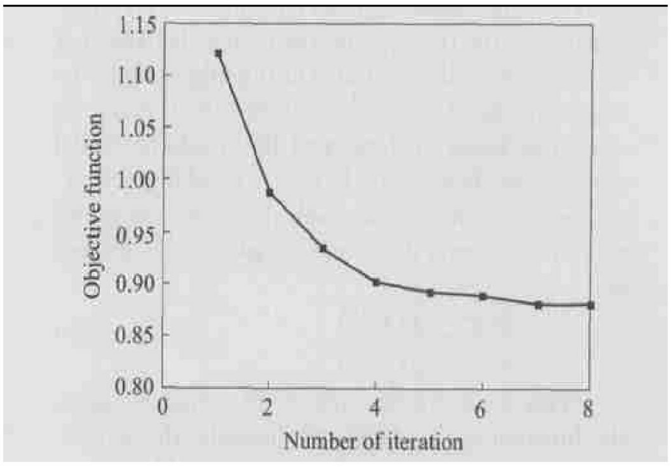

Fig. 7 Variation of objective function value

5 EXPERIMENTS

In order to verify the accuracy of this algor-

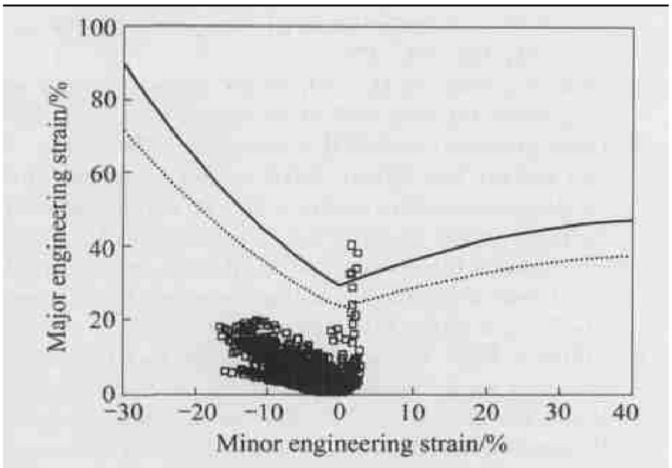

Fig. 8 Forming limit diagram(initial)

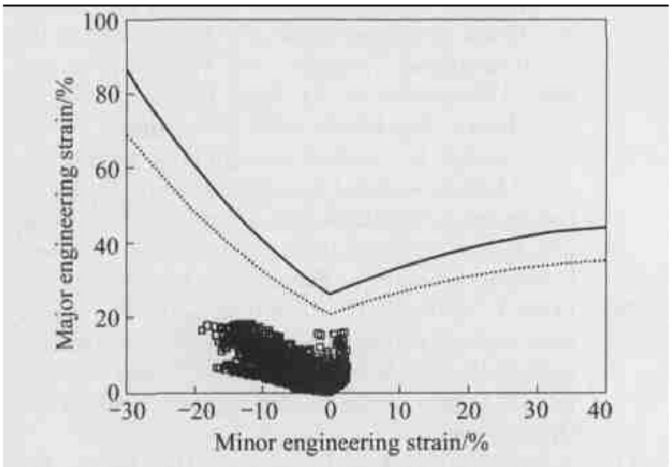

Fig. 9 Forming limit diagram(optimal)

ithm, the rectangular pan deep drawing experiments are performed on a multi-point variable blank-holder forces hydraulic press(Fig. 10) installed at the Auto-body Manufacturing Technology Center at Shanghai Jiaotong University. The blank-holder forces which can be kept constant or varied as a function of stroke and location are applied by means of a hydraulic cushion, with a maximum load of 60 kN. One-piece but relatively flexible blankholder is designed to control the BHF at different locations. Fig. 11 shows the schematic diagram of the blank holder used in these experiments. These tests were done in two series. At first, different constant blank-holder forces were applied, and then, the optimal variable blank-holder forces which were obtained from the results of described optimal algorithm were applied. The attainable pan height is also shown in Fig. 11.

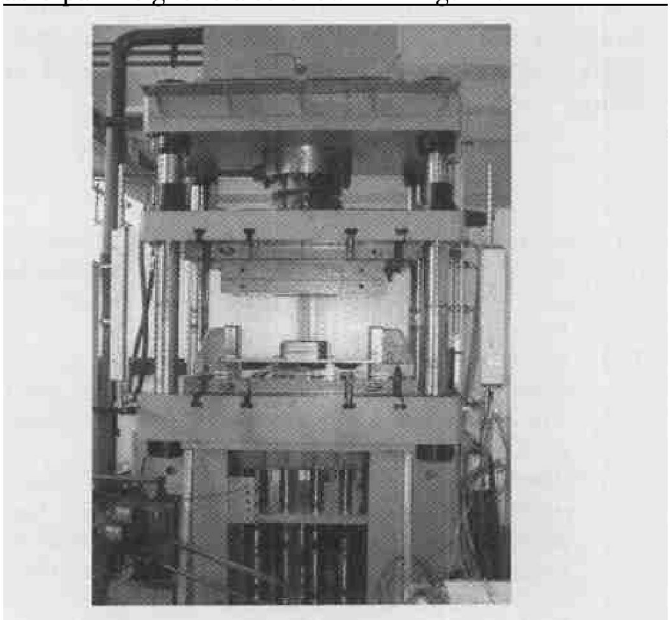

Fig. 10 Multi-point variable blank-holder forces hydraulic press

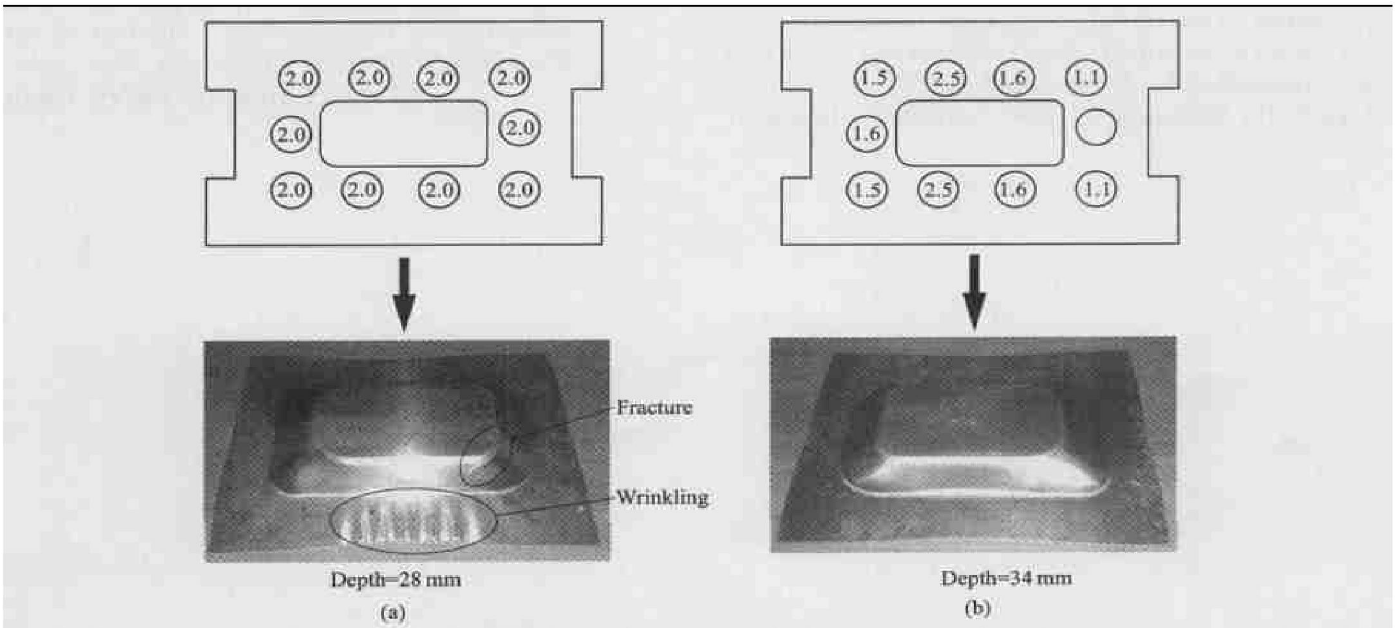

Fig. 11 Stamped parts under initial and optimal BHFs
(a) —Initial BHFs; (b) —Optimal BHFs

6 CONCLUSIONS

In this paper, a new optimization methodology is developed for determining the optimum BHFs with respect to the location in order to improve the formability of aluminum alloy sheet. The methodology incorporates the finite element analysis and simulation-based optimization scheme. The optimum variable blankholder forces which are very difficult to determinate during sheet metal forming were determined automatically by minimizing the objective function. Experimental results show that the obtained optimum variable blankholder forces can increase the depth of the aluminum alloy rectangular box. The numerical and experimental results confirm the validity of the presented algorithm.

REFERENCES

[1] Ahmetoglu M A, Altan T, kinzel G L. Improvement of part quality in stamping by controlling blankholder force and pressure[J]. Journal of Materials Processing Technology, 1992, 33: 195-214.

[2] Ahmetoglu M A, Broek T R, Kinzel G, et al. Control of blank holder force to eliminate wrinkling and fracture in deep-drawing rectangular parts[J]. Annals of the CIRP, 1995, 44(1): 247-250.

[3] Obermeyers J, Majlessi S A. A review of recent advances in the application of blank-holder force towards improving the forming limits of sheet metal parts[J]. Journal of Materials Processing Technology, 1998, 5: 222-234.

[4] WANG Xin-yun, WANG Zhong-jin, WANG Zhong-ren. Effect of blank holder pressure on viscous pressure forming aluminum alloy ladder parts[J]. Trans Nonferrous Met Soc China, 2003, 13(2): 391-397.

[5] WANG Zhong-jin, WANG Xin-yun, WANG Zhong-ren. Effect of blank holder pressure on viscous pressure forming aluminum alloy ladder parts[J]. Trans Nonferrous Met Soc China, 2002, 12(1): 109-114.

[6] Hayashi H, Nakagawa T. Recent trends in sheet metals and their formability in manufacturing automotive panels [J]. Journal of Materials Processing Technology, 1994, 46: 455-474.

[7] Huh H, Kim Se-Ho. Optimum process design in sheet-metal forming with finite element analysis[J]. Transactions of the ASME, 2001, 123: 476-481.

[8] Kim Se-Ho, Huh Hoon. BHF control algorithm with the design sensitivity analysis for the improvement of the deep drawn product[A]. Proceedings of the 5th International Conference and Workshop on Numerical Simulation of 3D Sheet Forming Processes[C]. Korea: Jeju Island, 2002. 121-126.

[9] Hillman M. Optimization of sheet metal forming processes using simulation programs[A]. Proceedings of the 4th International Conference and Workshop on Numerical Simulation of 3D Sheet Forming Processes[C]. Besancon, France, 1999. 13-176.

[10] Roy S, Kunju R, Kirby D. An automated and flexible approach to optimal design of shape and process variables for stamping parts[A]. Proceedings of the 5th International Conference and Workshop on Numerical Simulation of 3D Sheet Forming Processes[C]. Korea: Jeju Island, 2002. 573-578.

[11] Neddermeijer G, van Oortmarssen G J, Piersma N, et al. A framework for response surface methodology for simulation optimization [R]. Econometeris institution reports, EI2000-14/A. Netherlands: Erasmus University Rotterdam, Econometric Institute, 2000.

[12] Perez V M, Renaud J E, Watson L T. An interior point sequential approximate optimization methodology [A]. Proceedings of the 8th IAA/NASA/USAF/ISSMO Symposium on Multidisciplinary Analysis and Optimization[C]. Long Beach, CA, USA, 2002.

[13] Yang Jae-Bong, Joen Byung-Hee, OH Soo-Ik. Design sensitivity analysis and optimization of the Hydroforming process[J]. Journal of Materials Processing Technology, 2001, 113: 666-672.

[14] Rodrguez J F, Renaud J E, Wujek B A, et al. Trust region model management in multidisciplinary design optimization[J]. Journal of Computational and Applied Mathematics, 2000(124): 139-154.

[15] Morris M D, Mitchell T J. Exploratory designs for computational experiments[J]. Journal of Statistical Planning and Inference, 1995, 43: 381-402.

(Edited by PENG Chao-qun)